Elena M. Seftel, Jeroen Spooren, Monika Kus, Pegie Cool, Bart Michielsen, *Journal of Environmental Chemical Engineering* 12 (**2024**) 112196
https://doi.org/10.1016/j.jece.2024.112196

La-doped MgFe-Layered Double Hydroxides and their sorption properties towards Tungsten Oxyanions (WO_4^{2-}) at alkaline pH's

Elena M. Seftel*[,a], Jeroen Spooren[a], Monika Kus[a], Pegie Cool[b], Bart Michielsen[a]

[a]Sustainable Materials Unit, VITO Flemish Institute for Technological Research, Boeretang 200, B-2400, Belgium
elena.seftel@vito.be, jeroen.spooren@vito.be, monika.kus@vito.be, bart.michielsen@vito.be

[b]Laboratory of Adsorption and Catalysis, Department of Chemistry, University of Antwerp (CDE), Universiteitsplein 1, 2610 Wilrijk, Antwerp, Belgium, pegie.cool@uantwerpen.be

* corresponding author: elena.seftel@vito.be

Abstract

The present study focuses on the tungsten recovery from alkaline solutions using for the first time La-doped MgFe-LDH type sorbents (pH ≥ 13). A small-scale synthesis procedure was optimized, and further upscaled (20x) to produce up to 200g batches with reproducibility degree close to 100 %. The chemical composition, structural and textural characteristics of the as-synthesized materials were investigated by ICP-OES, X-ray Diffraction, N_2 physisorption and IR spectroscopy techniques. The materials were applied for sorption of WO_4^{2-} anions in aqueous media under relevant conditions. Parameters influencing the sorption process, such as the LDH composition, pH of the sorption media, adsorption capacity, kinetics and desorption solution composition were thoroughly investigated. Multi-cycling tests in different desorption solutions combined with IR and XRD characterization of the La-MgFe-LDH solids in different steps of the process, allowed us to elucidate the WO_4^{2-} recovery mechanism. Further, the La-doping in the LDH structure increases the sorption capacity and assures the material stability throughout the WO_4^{2-} recovery process in high pH media. The alkaline stability was demonstrated by powder post characterization by X-ray Diffraction as well as performing alkaline stability test and follow up of any leaching elements by ICP-OES in alkaline solutions. The results indicate that the as-developed La-MgFe-LDH are suitable candidates for WO_4^{2-} recovery from aqueous solutions, including highly alkaline solutions compatible with the current hydrometallurgical processes.

Keywords

Layered double hydroxides, structural modification by La-doping, alkaline stability, WO_4^{2-} recovery

1. Introduction

Tungsten is an important metal for many applications in various technological fields. Materials composed of, or containing tungsten are known to be very strong, durable and resistant to corrosion, as tungsten has a high density and the highest melting point of all metals [1, 2]. Tungsten is listed as a critical raw material (CRM) by the European Commission (EC 2023), mainly due to the high economic importance and its supply risk [3]. The economic importance of tungsten is determined by its low substitutability and the end-use applications such as drilling and mining materials, high-resistant steel and construction material for (fusion) reactors. Therefore, it becomes increasingly more important to recover or recycle tungsten.

Tungsten is refined from both mined tungsten rich ores and tungsten containing scraps [1, 4]. Both types require hydrometallurgical processing. These are based on leaching in acid and/or alkali solutions due to their very low water solubilities. In the old methods of hydrometallurgical processing were mainly using acid digestion for its conversion to tungstic acid. This was further dissolved in ammonium hydroxide and further crystallized in ammonium paratungstate (APT) [5]. However, in the modern hydrometallurgical process, all tungsten feeds are digested in sodium hydroxide or sodium carbonate, and the sodium tungstate (Na_2WO_4) that results after purification steps is converted to APT after the separation of sodium via liquid ion exchange. Also, digestion of tungsten-containing feeds are caried out in concentrated alkali solutions (NaOH and/or Na_2CO_3) to produce a mixture comprising soluble Na_2WO_4 and an insoluble sludge. The mixture is subsequently diluted to form an aqueous fraction containing dissolved Na_2WO_4, which is separated from an insoluble sludge fraction via filtration [6, 7]. These processes are typically followed by the purification of the sodium tungstate solutions. This is usually performed via solvent extraction in which a pH reduction step to acidic values is required. The solvent extraction uses various types of amines and the optimum extraction pH is between 1 to 5 [5, 7, 8].

Besides the above-mentioned solvent extraction, adsorption by using ion exchangers represents an appealing alternative since the use of organic solvents can be avoided. Furthermore, the adsorbents can reduce the high costs and energy consumption as well as the generated secondary waste products [9-11].

A state of the art analysis of adsorbents for tungsten recovery shows the potential use of biosorbents [12], multi-walled carbon nanotubes [13], natural clays [4] and biopolymer coated clays [14, 15], zeolite and fly ash [16, 17] and layered double hydroxides [18-20]. The adsorption of tungsten oxy anions using layered double hydroxides has been studied, but to the best of our knowledge, there has been no study focusing on the use of LDH for direct tungsten recovery from solutions with a high alkalinity. Furthermore, most of the reports are describing detailed studies of the tungsten anions adsorption process, while the desorption process is rather ignored. We believe that a focused evaluation on the desorption process with the tungsten recovery, LDH regeneration and its use for multiple cycles is of great importance for the progress in bringing LDHs closer to their application in industrial processes. Layered double hydroxides, also known as hydrotalcite (HT) compounds or anionic clays, are composed of positive charged layers and exchangeable anionic interlayer species [21-23]. The material is generally described by the chemical formula $[M^{2+}_{1-x}M^{3+}_{x}(OH)_2]^{x+}$ $(A^{n-}_{x/n})\cdot mH_2O$, where M^{2+} are divalent cations such as Mg^{2+}, Zn^{2+} and Ca^{2+} and M^{3+} are trivalent cations like Al^{3+}, Fe^{3+} and Mn^{3+}. The A^{n-} are the exchangeable anions (carbonates, nitrates, chlorides, etc.) located in the interlayer gallery together with water molecules. A large variety of LDHs with various compositions related with different combinations and ratios between the M^{2+}/M^{3+} and various interlayer anionic species exists [22, 24].

Among the various compositions reported in the scientific literature, the MgFe- and MgAl- show high potential and are worth to investigate for the tungsten anions uptake from aqueous media. For these compositions, high sorption capacity, different kinetics or anion competitive sorption when applied in mixed solutions has been reported. Noteworthily, these studies only refer to aqueous streams with a pH ranging from neutral to maximum pH of 11 and generally lack information on the material stability, regeneration and/or recyclability of the LDH sorbent material [4, 15, 18-20, 25]. An overview on the state of the art describing the use of LDHs for tungsten sorption is given in Table 1.

In this study we report for the first time on the development of an Fe-based LDH sorbent with an innovative structure by doping with La^{3+} cations within the brucite-type layers for tungsten recovery from aqueous solutions with high alkalinity (pH ≥ 13). A high adsorption capacity and preserved alkaline stability of the developed Fe-based LDH is ensured by La doping. Further, both the adsorption and the desorption steps were investigated and optimized to enable an efficient and eco-friendly tungsten recovery process which can be applied directly

in alkaline solutions. Therefore, the sorption process will be compatible with the current hydrometallurgical tungsten refining processes.

Table 1. Survey on the state of the art reporting the use of LDHs for tungsten uptake

Adsorbent	Focus of the study	W adsorption				W desorption			Observations	Ref.
		Optimum pH / pH range studied	W species	q_{max}, mg/g (at RT)	q_{max} at pH 13 mg/g (at RT)	Desorption solution	Desorption efficiency	No. of cycles		
MgFe-LDH Pyroaurite-type Mg/Fe = 3, 4, 5 $A^{n-} = NO_3^-$	Determination of adsorption capacity for W	3 – 11 / 2 - 13	Polyoxoanions (as a function of pH)	56.5 (pH 3 – 11)	~5	-	-	-	Dissolution of LDH at very low pH (pH2) and very high pH (pH12-13)	[19]
MgFe-LDH Pyroaurite-type Mg/Fe = 3, 5 $A^{n-} = Cl^-$	Study of influence of Mg/Fe ratio on W sorption	2 / 2 - 10	Polyoxoanions (as a function of pH)	30 – 60 (as a function of pH)	-	NaOH 1, 10 and 100mmol/L	15 – 30% as a function of NaOH concentration 24h	1	Dissolution of LDH at very low pH (pH2). At pH 10 – competition with HO^- ions	[18]
MgFe-LDH Iowaite-type Mg/Fe = 2, 2.5 3 $A^{n-} = Cl^-$	Removal of tungstate from aqueous solutions	3 – 11 / 2 - 13	Polyoxoanions, (as a function of pH)	54.1 (pH 3-11)	~3.5	0.004 - 0.04% NaOH solutions	Up to 77.3% using 0.04%NaOH 24h	1	Dissolution of LDH at very low pH (pH2). At pH 10 – competition with HO^- ions and dissolution of LDH	[4]
MgFe-LDH non-delaminated Mg/Fe = 3 $A^{n-} = NO_3^-$	W removal from water	4 -10 / 2 - 12	Polyoxoanions (as a function of pH)	57.3	-	-	-	-		[15]
MgFe-LDH delaminated Mg/Fe = 3 A^{n-} = L-asparginine	W removal from water	4 -10 / 2 - 12	As a function of pH	90.5	-	-	-	-		[15]
MgAl-LDH Mg/Al = 3 $A^{n-} = CO_3^{2-}$	W extraction from aqueous solutions	4 - 8	$W_7O_{24}^{6-}$	1 – 8.5 (as a function of pH)	-	Na_2CO_3 pH 10	50% to 100% depending on desorption time (up to 120h) and adsorption pH	1		[20]
ZnAl-LDH Zn/Al = 3 $A^{n-} = CO_3^{2-}$, SO_4^{2-}	Spectroscopic study of W adsorbed species onto LDH surface	5.5	$W_7O_{24}^{6-}$	-	-	-	-			[25]

MgFe-LDH Mg/Fe = 3 $A^{n-} = NO_3^-$	W recovery at high alkaline pH (pH ≥ 13)	6.2 - 13	WO_4^{2-}	41	4	-	-	-		This study
La-doped MgFe-LDH Mg/Fe = 3 $A^{n-} = NO_3^-$	W recovery at high alkaline pH (pH ≥ 13)	6.2 - 13	WO_4^{2-}	56	11	NaOH (0.1M – 1M), 1M NaCl, 1M $NaNO_3$ or 1M Na_2CO_3	~95% in 1M NaOH	3	Adsorption / desorption efficiency maintained during 3 repeated cycles	This study

2. Materials and methods

2.1. Synthesis of LDH materials

The La-doped Fe-LDH materials were synthesized using the co-precipitation method and nitrate as the interlayer anion according to an earlier described synthesis method. An optimized automatic titration procedure was used to perform the coprecipitation reaction which uses aqueous ammonia solution to rise the pH of the nitrate salts and maintain it at a constant value of 11. The ammonia co-precipitation agent was used as it facilitates the intercalation of nitrate anions within the interlayer gallery of LDHs, without the necessity of using boiled solutions along with inert atmosphere to prevent CO_3^{2-} incorporation in the interlayer [26, 27]. In this synthesis procedure, a 100mL of 1M mixed nitrate salts solution of Mg^{2+}, Fe^{3+} and La^{3+} was used ($Mg(NO_3)_2.6H_2O$ ACS reagent 99%, $Fe(NO_3)_3.9H_2O$ ACS reagent ≥98% and , $La(NO_3)_3.6H_2O$ Sigma Aldrich 99,9%) in which the molar ratio M^{2+}/M^{3+} was fixed at 3/1, and that of Fe^{3+}/La^{3+} at 0.9/0.1. To this solution, an ammonia aqueous solution (25%, EMSURE® for analysis, Supelco®), was added under continuous stirring at 25°C, until the pH was raised and maintained constant at pH 11. The obtained slurry was aged for 24h under continuous stirring at 25°C. No inert gas, such as argon or nitrogen, was bubbled through the reaction mixture, neither during the coprecipitation or aging time. The precipitated product was separated by vacuum filtration, washed thoroughly with distilled water and dried at ambient conditions. The obtained material is denoted as La-MgFe-LDH [28].

The above-described method allowed us to obtain batches of powders of ~5-10 g, and it was further upscaled to obtain up to 200 g of powder with high reproducibility degree, of close to 100 %. The obtained powders are characterized by a broad particle size distribution. Therefore, the powders were sieved using a 0.45 µm sieve, and the finest fraction of particles with sizes below 0.45 µm was used to perform the W sorption testing. The particle size distribution and XRD of several upscaled batches are included in **Figure S1 and Figure S2** ***(SI file).***

2.2. Alkalinity stability testing

The alkaline stability of the obtained powders was tested in aqueous solutions with high alkalinity, e.g. pH ≥ 13. In a typical experiment, the materials were immersed in NaOH solutions of 1 M and 5 M for 2 h at a solid to liquid ratio (S/L) of 10 (g/L), and the evolution of the metals leaching were measured by Inductively Coupled Plasma – Optical Emission Spectroscopy ICP-OES. For these tests, standard MgAl-LDH (Pural MG63HT, Sasol GMbH) was

used as benchmark material. The obtained ICP results (**Figure S3, *SI File***), indicate that Al was leached from the commercial LDH (Pural MG63HT), while the La-doped LDHs powders were stable in alkaline media.

2.3. Batch adsorption experiments

Batch sorption experiments were carried out using $Na_2WO_4 \cdot 2H_2O$ (Sigma Aldrich, ≥ 99.0% purity) at a fixed solid to liquid ratio of 1 g/L. The experiments focused on the investigation of the influence of the LDH composition, influence of pH [29] on the adsorption kinetics, e.g. analysis of adsorbed concentration in time, and isotherms, e.g. determination of the maximum adsorption capacity and mechanism. To study the influence of the structural composition and select the optimum LDH composition, a sorption test was performed using an initial tungsten concentration of 100 mg W/L at short contact time (5 min) and longer contact time (120 min) as a function of pH. NaOH was used to increase the solution alkalinity up to pH ≥ 13. Adsorption kinetics of tungstate were evaluated by mixing the LDH adsorbents with tungstate solutions (solid/liquid ratio of 1 g/L) with a concentration of 100 mg W/L and sampling aliquots at selected time intervals. Adsorption isotherms were determined by mixing 1 g LDH/L of tungstate solutions with various concentrations ranging from 10 mg W/L to 200 mg W/L and 24 h stirring. The samples were separated with a 0.45 µm membrane filter, and the remaining tungsten concentrations were determined by ICP-OES measurements.

2.4. Batch desorption experiments

Desorption studies, e.g. elution in different desorption solutions, were done by taking 1 g/L of LDH sample in a syringe with membrane filter attached (pore size of <0.45 µm). First an adsorption step was performed with 100mgW/L solution at pH 13 and contact time for 120min. Then the W-loaded LDH was mixed with the desorption solution and shaken for 15min. The solution was filtered, and W solution was analyzed using ICP-OES. This sequence of steps were repeated for 3 times for the multi-cycling tests.

As desorption solutions, NaOH of various concentrations was used, namely 0.01M, 0.1M and 1M. To study the influence of addition of salts, desorption solutions combining 1M NaOH/1M NaCl, 1M NaOH/1M $NaNO_3$ or 1M NaOH/1M Na_2CO_3 were used. Due to the presence of salts in the desorption step, also a washing step with 0.1M NaOH was performed before starting the next adsorption/desorption cycle. All experiments were performed multiple times and error bars were provided.

2.5. Characterization techniques

2.5.1. X-ray diffraction

XRD patterns were recorded on a PANalytical X'Pert PRO MPD diffractometer with filtered CuK_α radiation; measurements were done in the 2θ mode using a bracket sample holder with a scanning speed of 0.04°/4 s in continuous mode.

2.5.2. Porosity and surface area determination by N_2 sorption

Studies by **N_2 sorption** were performed on a Quantachrome® ASiQwin™ automated gas sorption system using nitrogen (N_2) as the adsorbate at liquid nitrogen temperature (−196 °C). Prior to the measurements, an outgassing step was performed under vacuum for 48 h at 60°C. The surface area was calculated using the BET method in the range of relative pressure 0.05–0.35.

2.5.3. Particle Size Distribution

The powders particle size distribution (PSD) was determined through laser diffraction analysis technique using a Microtrac S3500. Each sample was measured 3 times, for 30 s with the flow rate at 55 % of the maximum flow.

2.5.4. Infrared spectroscopy

To detect the IR-active vibrational modes, a Thermo Nicolet spectrometer was used, equipped with a Platinum ATR module. A number of 200 scans were taken with a resolution of 4 cm^{-1}.

2.5.5. ICP-OES

An Agilent Inductively Coupled Plasma – Optical Emission Spectrometer type 5100 Vertical Dual View was used to determine the concentration of W and other elements in the aqueous solutions.

2.5.6. CHNS analysis

The CHNS measurements involves a high-temperature combustion at 1150°C under oxygen atmosphere and thermal conductivity detection. The CHNS measurements were performed with the vario EL cube element analyser (Elementar).

3. Results and discussions

The present study focuses on the development of La-doped Fe-based layered double hydroxides to recover tungsten oxyanions from aqueous media with high alkalinity. Fe-based LDHs compositions were selected as promising for tungsten oxyanions uptake based on the reported literature in this field [4, 15, 18-20]. All these reports are dealing with the application

for tungsten adsorption from neutral to slightly alkaline media (pH 5 to 11) and indicate that a further increase of the pH to values above 12 are leading to a major decrease in adsorption performances. On the other hand, the LDH stability as a function of pH is not really taken into consideration, only limited reports are describing the dissolution of the LDH matrix at very low pH (pH 2) or very high pH (pH 12 – 13) values, respectively [18, 19, 30].

The present study focuses on the development of an alkaline stable LDH adsorbent applicable directly in these high pH aqueous streams, such as the hydrometallurgical refining and recycling tungsten containing streams. At a first instance, the LDH matrix containing Mg and Fe is selected as a suitable LDH composition for selective sorption of tungsten oxyanions, as well as for its stability in alkaline media. Further, for their application in high alkaline media, we have doped the MgFe-LDH with La^{3+} cations to increase its alkaline stability and maintain the tungsten sorption properties, resulting in the material referred to as La-MgFe-LDH.

3.1 Composition and structure

Structural characterization performed by X-ray diffraction (**Figure 1**) indicates the presence of a well-defined crystalline structure with the characteristic reflections associated to layered double hydroxides. Namely, the appearance of the basal planes (003) and (006) at low 2θ angle and of the non-basal planes (101), 015), (018) and (110) at higher 2θ angles, respectively. No other additional phases could be detected, which is especially important for the La-doped MgFe-LDH material, indicating the successful incorporation of the La^{3+} cations within the brucite-like sheets. It should be noted that the incorporation of La^{3+} cations within the brucite-like layers by the partial isomorphous substitution of the Fe^{3+} cations is not favoured. An octahedral coordination is usually adopted in the brucite-like sheets of LDH-type networks, and the size of the octahedra in the LDH sheets is, to a certain extent, controlled by the size of the divalent cations, such as Mg^{2+} (ionic radius of 0.75Å). The Fe^{3+} ions have even a smaller ionic radius (0.64 Å) and the preferential adopted coordination number is 6 [21]. The La^{3+} ions of higher ionic radii (1.36 Å) have higher coordination number ranging from 7 to 10 [31], thus the isomorphic substitution of Fe^{3+} with La^{3+} cations in a MgFe-LDH is not favourable, and introduces distortions and defects in the brucite-type layer structure. Previous attempts in La^{3+} incorporation into the brucite-type layers of LDHs, even in lower degrees as reported in the present study, indicated the segregation of the $La(OH)_3$ phase on the surface of the LDH sheets. Y. Guo et al. [32] associated this $La(OH)_3$ segregation with the formation of the carbonate and oxy-hydroxide lanthanum species at the early stage of the

coprecipitation reaction during LDH synthesis. E. Rodrigues et al. [33] reported attempts to incorporate lanthanide ions within the LDH structure. Similarly, the strong ionic character of lanthanum leading to high anionic affinity favoured formation of carbonate species in very early stages of coprecipitation and in corroboration with its high ionic radius prevented intercalation of larger lanthanum species within the brucite-type layers and thus observing the segregation of $La(OH)_3$ and $LaCO_3OH$ in the XRD patterns. It should be noted that all these attempts to synthesize La containing LDHs are using NaOH / Na_2CO_3 coprecipitation solutions. Thus, the successful incorporation of the La^{3+} cations within the brucite-like LDH layers is here reported for the first time. The successful isomorphous substitution was enabled by involving ammonia alkaline solution during the coprecipitation step which inhibits the formation of the carbonate and oxy-hydroxide lanthanum species at the early stage of the coprecipitation reaction allowing its isomorphous substitution within the brucite-type sheets. This is based on the coordination chemistry of metal ions in the presence of ammonia ions, which first coordinate with the ammonia present in solution forming $[M(NH_3)_n]^{2+}$ or $[M(NH_3)_n]^{3+}$ complexes [34, 35]. This is followed by their slow release to the basic solution to yield LDH type hydroxide particles. A general scheme of this mechanism is illustrated below:

$$M^{2+} / M^{3+} + 2nNH_3 \rightarrow [M(NH_3)_n]^{2+} / [M(NH_3)_n]^{3+} \cdots + 2HO^- \cdots \rightarrow [M^{2+}M^{3+}(OH)_2] + 2nNH_3$$

Similarly, the carbonate anions, if present in the aqueous solutions, undergo complexation by ammonia and as a result they stay in the solution and inhibits their intercalation in the LDH interlayer space, thus favouring the formation of nitrate intercalated LDHs [36].

Therefore, the use of the ammonia synthesis route results into a nitrate intercalated La-MgFe-LDH under normal atmospheric conditions, without the requirement of inert atmosphere or other special synthesis conditions for avoiding the carbonate intercalation within the interlayer gallery [26, 27]. The CHNS analysis, used to investigate the nitrogen and carbon, showed that the obtained materials contain mainly nitrogen, while only traces of carbon could be detected (Table 2). This is very important for the anionic exchange properties and their use in the tungsten recovery process.

Table 2 includes the calculated values of the unit cell parameters obtained from the XRD characterization as well as the porosity, specific surface area and pore volume, measured using N_2 sorption characterization technique.

It may be observed that the value of the unit cell parameters ***a***, related with the cation-cation distance within the brucite-like sheets, is increasing upon La^{3+} doping indicating the successful isomorphous substitution of the La^{3+} cations within the brucite-like sheets. Further, the value of the unit cell parameter ***c*** is also higher after La^{3+} doping, as compared with the non-doped LDH, suggesting the increase of the thickness comprised of a brucite-like layer and the interlayer space, respectively. This increased value may be well correlated with an expected increase of the brucite-like sheets thickness based on the higher ionic radius of La^{3+}. Further, an increased interlayer population with nitrates may be also expected as the amount of intercalated nitrate anions is assumed to increase due to the incorporation of the La^{3+} which contributes to the total positive surface charges. This conclusion correlates well with the increased adsorption capacity of the La-MgFe-LDH obtained during the WO_4^{2-} adsorption study, as it will be highlighted in the following sections. Additionally, we have performed the CHNS analysis on the synthesized LDHs, which demonstrated the increase of the N content in the case of La-MgFe-LDH.

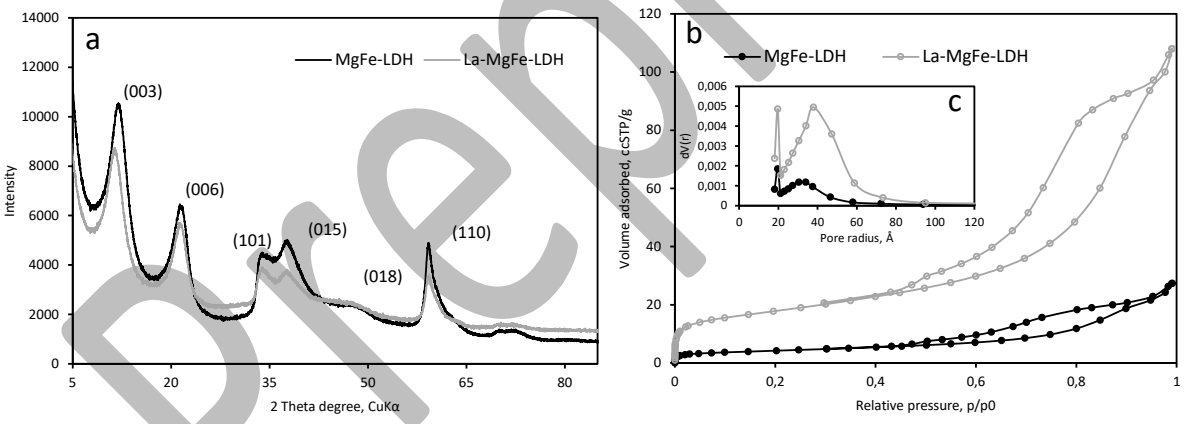

Figure 1. X-Ray diffraction patterns of (a) and porosity characterization by N_2 adsorption-desorption isotherms (b) with BJH pore size distribution (c) of the MgFe-LDH and La-MgFe-LDH materials.

Table 2. Details on composition, structural parameters and porosity of the synthesized LDHs.

Sample	*x*	Mg^{2+}/Me^{3+} (molar ratio)	N (mol)	C (mol)	Calculated chemical formula of the brucite-like sheets	S_{BET} (m^2/g)	V_p (cm^3/g)	Unit cell parameters	
								***a*, Å**	***c*, Å**
MgFe-LDH	0.247(6)	3.038(8)	0.19(3)	0.02(2)	$Mg_{0.752}Fe_{0.246}$	15	0.037(6)	3.10	23.9
La-MgFe-LDH	0.238(0)	3.200(2)	0.20(8)	0.02(1)	$Mg_{0.762}Fe_{0.214}La_{0.024}$	65	0.155(1)	3.12	24.2

x = $M^{3+}/(M^{2+}+M^{3+})$ molar ratio and chemical formula calculated from ICP-OES measurements; N and C (mol) determined by CHNS analysis, S_{BET} – specific surface area and Vp – pore volume measured by N_2-physisorption, ***a*** and ***c*** – unit cell parameters ***a*** = $2d_{110}$, ***c*** = $3d_{003}$

As the measurements for the specific surface area by N_2-physisorption characterization technique indicate that the porosity characteristics are also affected by the presence of the La^{3+} ions doped within the brucite-like sheets (see **Table 2**), which is an important characteristic when dealing with an adsorption process. Namely, the La-doping into the MgFe-LDH structure leads to increased specific surface area as well as pore volume. The shape of the isotherms typically assigned to Type IVa with a H_5 hysteresis shape (**Figure 1b**) [37]. The two-step delayed desorption at relative pressures $p/p_0 > 0.4$ indicates the presence of bimodal porosity, the size of mesopores also observed form the BJH pore size distribution indicating pores with sizes in the range of 40Å and larger mesopores with a broader size distribution between the ranges of 40Å to 80Å (**Figure 1c**).

3.2. W (WO_4^{2-}) adsorption study

Sorption performance is influenced by the type of metals isomorphously substituted in the brucite-like sheets (e. g. Mg^{2+}, Fe^{3+} or La^{3+}) and the intercalated anion, e.g. nitrate anions (NO_3^-) which can be easily exchanged with the tungstate anions (WO_4^{2-}) [25]. On the other hand, it is expected that the sorption capacity is decreasing by increasing the pH due to multiple factors. At first, surface charge changes should be considered, as the pH influences the isoelectric point of the LDH as well as the speciation of the tungsten species. At pH 13 the tungsten is present in aqueous solutions as a divalent oxyanion (WO_4^{2-}) [25] which can directly interact with the positively charged surface of LDHs. Furthermore, doping with La^{3+} cations is contributing to the total positive surface charges, enabling the WO_4^{2-} sorption, as compared with an undoped MgFe-LDH.

The La-doping into the structure also enhances the alkaline stability and inhibits its dissolution in the sorption media, as usually observed with state-of-the-art LDH compositions [38, 39]. However, at pH 13, the solution is highly alkaline, which can lead to the formation of carbonate and hydroxide ions from dissolved CO_2 and water, respectively. These anions can compete with the WO_4^{2-} ions for sorption sites on the LDH surface and reduce the adsorption of WO_4^{2-} [22, 24].

In the present study, taking into account that different LDH compositions were prepared, the adsorption study was conducted first by a screening of the sorption performance as a function of LDH composition followed by a more detailed investigation of one selected composition which performs best in terms of adsorption capacity and kinetics, especially in W containing solutions with high alkalinity (pH 13).

3.2.1. Screening of LDH composition for W adsorption

The screening of LDH composition for W adsorption as a function of pH is shown in **Figure 2**. At both pH values tested, the La-MgFe-LDH material shows better WO_4^{2-} adsorption performances as compared with the non-doped MgFe-LDH, and this can be correlated with the different sorption sites induced by the presence of the La^{3+} cations within the LDH sheets as well as higher specific surface area as discussed in the previous section. An indication on the kinetic behaviour was also obtained from these screening tests. Short and long contact times were followed in these first screening tests to obtain information on the kinetics (at short contact time) as well as on the sorption capacity (longer contact time), respectively. The adsorbed WO_4^{2-} within 5 min of contact time reaches almost the full adsorption capacity of both LDH compositions indicating thus the high rate for WO_4^{2-} adsorption. In the case of non-doped MgFe-LDH, although at low pH of the sorption media a slight increase of maximum adsorbed tungsten is observed at a longer contact time, its adsorption capacity at pH ≥ 13 remains ~4 mg W/g even at a prolonged contact time. La-doping within the La-MgFe-LDH structure increases the adsorption capacity to ~11 mg W/g (**Figure 2**).

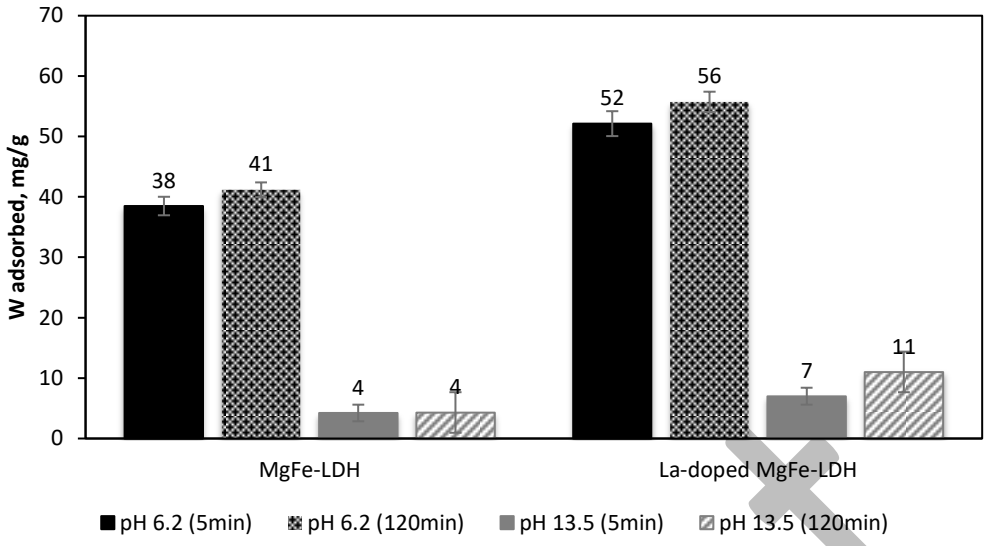

Figure 2. Screening of W adsorption efficiency as a function of pH on different LDH compositions (RT, Ci = 100mg/L, S/L = 1g/L, contact time = 5min or 120min).

These results are in accordance with the measured adsorption capacity at pH 13 determined by analysing the adsorption isotherms on both LDH materials, non-doped and La-doped, respectively (**Figure 3**). The obtained results demonstrate that the presence of La^{3+} cations doped within the structure of the La-MgFe-LDH material increases the sorption capacity as compared with the non-doped MgFe-LDH correspondent.

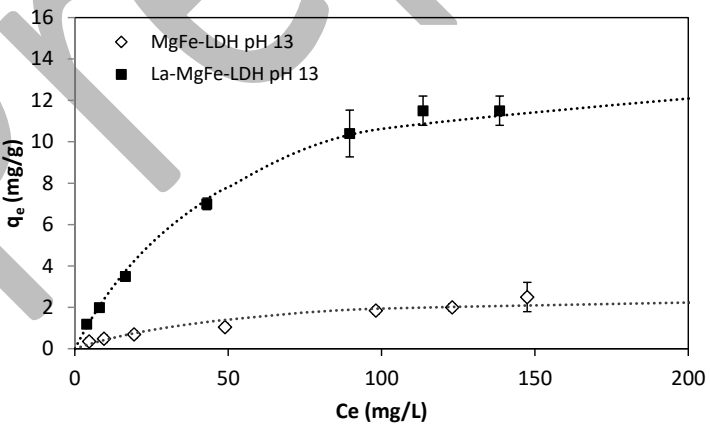

Figure 3. Determination of the adsorption isotherms on MgFe-LDH and La-MgFe-LDH at pH 13 (RT, S/L = 1g/L, contact time = 120min).

From these preliminary W adsorption data we selected the La-MgFe-LDH material for further testing. Larger batches of the La-MgFe-LDH material were synthesized (e.g. of 200g), and the

corresponding XRD characterization of the upscaled samples can be visualized in **Figure S2**. The X-ray diffraction patterns indicate the successful transfer of the synthesis protocol to larger scale (20x) of the LDH with tailored structure doped with La^{3+} cations, which is for the first time demonstrated and reported up to our knowledge.

The chemical composition of the obtained LDH samples were analysed using ICP-OES (**Table S1**).

3.2.2. Influence of pH on the adsorption isotherms

The results of tungsten sorption isotherm experiments as a function of pH are presented in **Figure 4.**

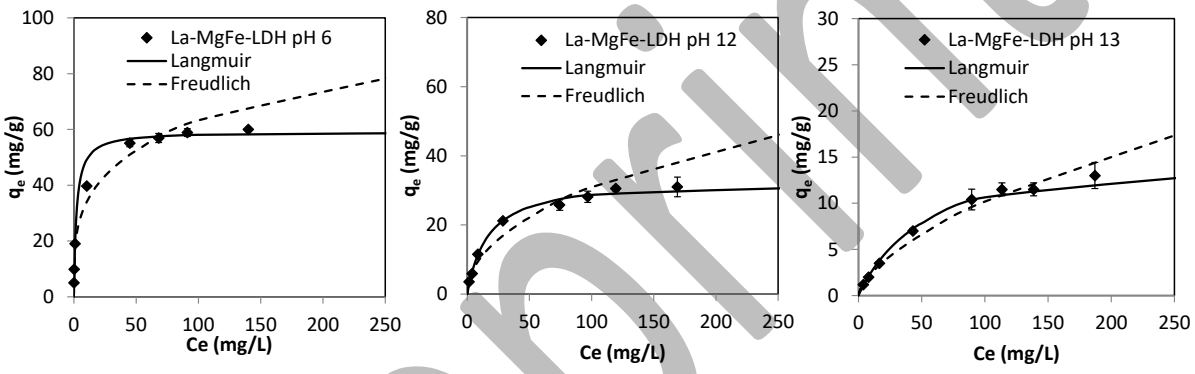

Figure 4. Adsorption isotherms and modelling of tungstate on the La-doped MgFe-LDH as a function of pH (RT, S/L = 1g/L, contact time 120min).

The adsorption data were fitted using the Langmuir and Freundlich models [22, 40, 41] to describe the relationship between the WO_4^{2-} concentration in solution and the amount of WO_4^{2-} species adsorbed onto the LDH surface. The Langmuir isotherm model assumes that the adsorption takes place at specific sites on the surface and that the adsorption rate is proportional to the concentration of the solute in the solution [22, 41]. The Freundlich isotherm model assumes that the adsorption takes place on a heterogeneous surface and that the adsorption rate is proportional to the concentration of the solute raised to a power [22, 40]. The adsorption data obtained at pH 6 and pH 12 fit well with the Langmuir model, while at pH 13 a combination of both Langmuir and Freundlich models might apply, as the correlation coefficients obtained by the 2 models are both very close to 1 (**Table 3**). This could be an indication that at pH 13, two competing processes e.g., anion exchange and/or surface electrostatic attraction between the WO_4^{2-} at the different adsorption sites based on the LDH

composition, e. g. Mg – OH, Fe – OH or La – OH sites. These aspects will be discussed in the later section when the desorption study is performed in various desorption solutions to effectively study the regeneration behavior and WO_4^{2-} elution from the different M – OH sites.

Table 3. Isotherm parameters for W adsorption onto La-MgFe-LDH at various pH's.

Adsorption pH	**Langmuir isotherm model** $q_e = K_L q_{max} C_e / (1 + K_L C_e)$			**Freundlich isotherm model** $q_e = K_F C_e^n$		
	q_{max} (mg/g)	**K_L**	**R^2**	**K_F**	**1/n**	**R^2**
pH 6	59.3	0.469(6)	0.998(7)	27.805	0.165	0.943(4)
pH 12	33.9	0.058(2)	0.994(1)	3.460(9)	0.462	0.963(3)
pH 13	16.6	0.017(6)	0.994(4)	0.559(9)	0.629	0.986(8)

K_L and K_F represent the Langmuir bonding term related to interaction energies (L/mg) and the Freundlich affinity coefficient ($mg^{(1-n)}L^n/g$), respectively, q_{max} denotes the Langmuir maximum capacity (mg/g), q_e denotes the amount adsorbed at equilibrium (mg/g), C_e is the equilibrium solution concentration (mg/L) of the sorbate and *n* is the Freundlich linearity constant

It should be also considered that, in the case of layered double hydroxides, the pH influences the charge on the LDHs surface and thus the adsorption behaviour. LDHs are anionic clay minerals having a positively charged layer and interlayer region containing the exchangeable anions, e. g. the NO_3^- in the present case. At low pH, the surface charge of the LDHs becomes more positive due to protonation of the hydroxyl groups on the layer surface. This leads to an increase in the adsorption of negatively charged species due to enhanced electrostatic attraction between the positively charged LDH layer and the negatively charged WO_4^{2-} species. However, at high pH, the LDHs become negatively charged due to deprotonation of the hydroxyl groups on the layer surface. This can lead to a decrease of the negatively charged WO_4^{2-} species, respectively.

3.2.3. Adsorption kinetics

The results of tungsten sorption kinetic experiments as a function of initial concentration at high pH , are shown in **Figure 5**.

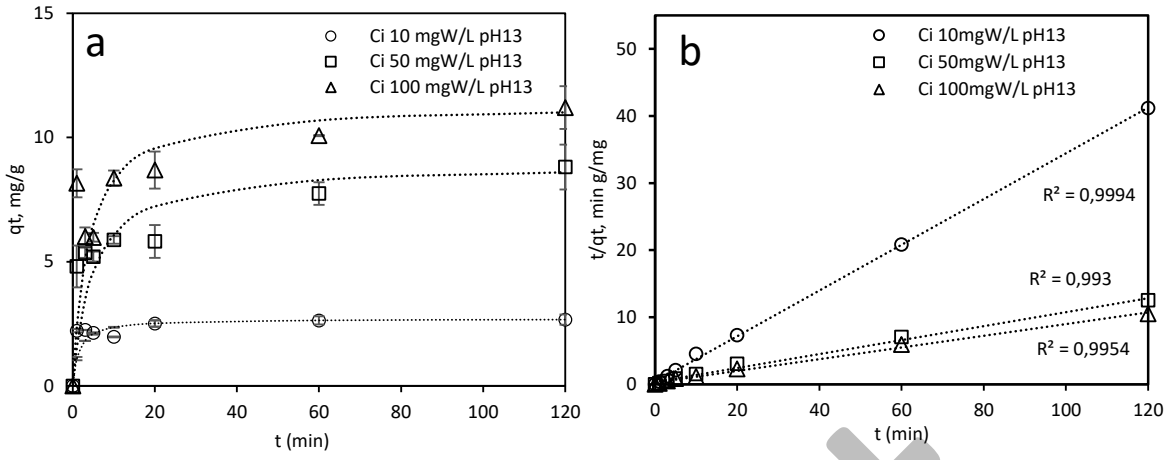

Figure 5. Adsorption kinetic data as a function of initial W concentration at pH 13, as well as the representation of the kinetic modelling using the pseudo-second order kinetic model.

These results show that the adsorption degree (mg W/g) is rapidly increasing in time in all cases and that the equilibrium is reached differently as a function of the initial concentration. Increasing the initial concentration leads to an increased adsorbed WO_4^{2-} to the solids, but also a slight delay in reaching the equilibrium, e. g. 1 – 3 min at 10 mg W/L while nearly 60min up to 2 h at 100 mg W/L, respectively. At lower W initial concentrations, the adsorption sites are readily available to favour the adsorption process. At higher initial W concentrations, the adsorption sites are filled in gradually, e.g. firstly the surface and then the interlayer, leading to overall slightly slower adsorption kinetics. The data was fitted using different kinetic models [42-45], from which the pseudo-second order (PSO) model fits best, and its representation is included in **Figure 5**. It also correlates well and demonstrates that the rate of adsorption is the highest in case of low initial W concentration, e. g. for initial concentration (Ci) of 10 mg W/g, while rather similar for higher initial concentrations. Strong correlations for data (**Table 4**) and agreement between experimental and calculated adsorption capacity (q_e) data suggest that this model represents W adsorption extremely well.

Table 4. Kinetic parameters of W adsorption onto La-MgFe-LDH at various initial pH and W concentrations.

Model	**Parameter**	**pH 13**		
		Ci 10 mg W/L	Ci 50 mg W/L	Ci 100 mg W/L
Experiment	q_e, mg/g	2,92	9,60	11,45
Pseudo-first order (PFO) $\ln(qe - qt) = \ln(qe) - \frac{k_1}{2.303}t$	q_e, (mg/g)	0,803(9)	4,709(1)	5,286(7)
	k_1 (min^{-1})	0,050(3)	0,025(4)	0,027(7)
	R^2	0,736(1)	0,766(8)	0,671(1)
Pseudo-second order (PSO) $\frac{t}{qt} = \frac{1}{k_2 qe^2} + \frac{t}{qe}$	q_e, mg/g	2,699(8)	8.9366	11.350(7)
	k_2, g/mg.min	0.253(3)	0.023(6)	0.023(5)
	R^2	0,999(4)	0,993(0)	0,995(4)
Elovich $qt = \frac{1}{b}\ln(ab) + \frac{1}{b}\ln(t)$	a, mg/g.min	6,03E*10^6	1,52E*10^2	8,64E*10^2
	1/b, mg/g	8,620(7)	1,225(6)	1,110(5)
	R^2	0,545(8)	0,864(8)	0,617(2)

Ci is the initial concentration, q_t and q_e are the amount of W adsorbed (mg/g) at time t and at equilibrium, respectively; k_1 and k_2 are the apparent adsorption rate constants, a and b are constants of the Elovich equation; constants in pseudo-second order and Elovich equations are calculated without using q_0 (t = 0, q_0 = 0)

3.3. W (WO_4^{2-}) desorption study and multi-cycling experiments

The regeneration and reuse of LDH after the adsorption step is of high importance as it can provide a cost-effective and sustainable solution for metal recovery or removal from various streams. Thus, the recycling performance, by means of desorption degree as well as possibility to use in multicycle steps, is critical to optimize. The regeneration of LDHs is important as it can restore their adsorption capacity. Further, their reuse for multiple cycles may significantly reduce the costs as well as the environmental impact associated with their synthesis and disposal.

Different solutions were reported as optimum regeneration solutions to eluate the adsorbed species (arsenates, phosphates, tungstates,…) from LDHs matrices: NaOH [18, 46-48], NaCl [48], $NaNO_3$ [48], $NaHCO_3$ or Na_2CO_3, Na_2HPO_4 [48], or combinations of NaOH and the forementioned salts [20, 38, 47], at various pH values. In some cases, regeneration is achieved in very high degree (~> 90%), but sometimes, efficiencies below 40% are obtained [48].

Therefore, the regeneration process has to be designed case by case, as a general procedure does not exist.

Taking into account all these findings, we used alkaline solutions of NaOH at various concentrations, and combined with various salts to optimize the desorption protocol and enable multi-cycling. Moreover, these efforts will provide us with additional information on the adsorption mechanism, taking into consideration that the tungsten species might adsorb on different sorption sites as suggested by the conclusions drawn from the modeling of the kinetic and isotherm data in previous sections.

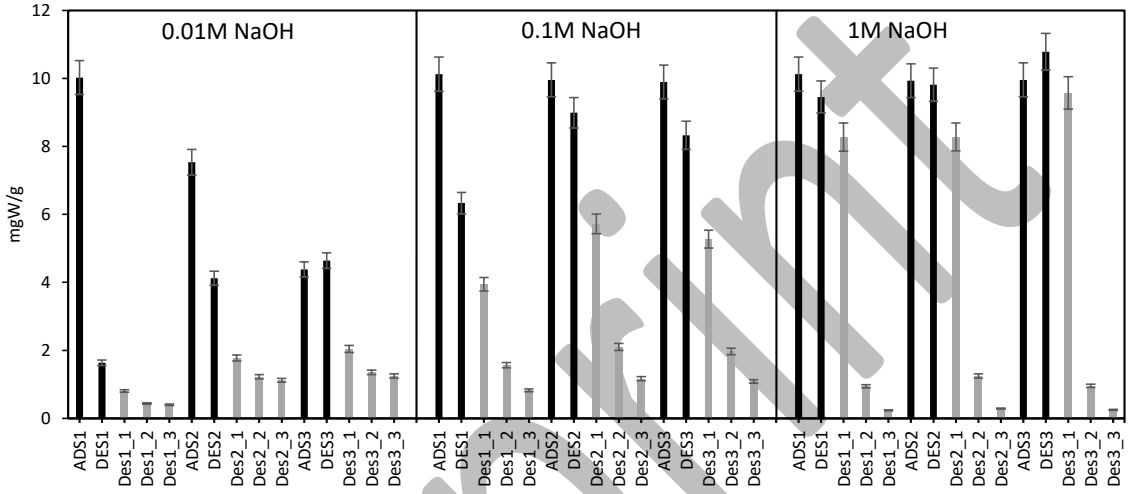

Figure 6. Desorption study in NaOH solutions at various concentrations, where ADS stands for adsorption step (RT, S/L = 1g/L, contact time 120min and Ci of 100mgW/L) and DES stands for the desorption step (RT, S/L = 1g/L, contact time of 15min).

The desorption performances in NaOH solutions were tested for 3 consecutive adsorption/desorption cycles and as a function of NaOH concentration. During the desorption process, NaOH is added to the LDH suspension and stirred for 5min and repeated 3 times (e.g. the grey bars in **Figure 6**, where Des1_1 stands for desorption cycle step 1 in NaOH solution for 5 min) to ensure complete desorption.

The results show that the NaOH can effectively break the electrostatic interactions between the LDH layers and the intercalated WO_4^{2-} anions, leading to their release into the desorption solution.

It is interesting to see that at low NaOH concentrations, multiple desorption steps are required to desorb the tungstates, as denoted with DES1 of a total duration of 15min (**Figure 6,** black bars), and represents the sum of 3 consecutive steps of 5 min analyzed separately,

denoted with D1_1, D1_2 and D1_3 (**Figure 6,** grey bars). But even if repeating this 5min desorption step for 3 times with lower NaOH concentration, it is not resulting in complete desorption degree as when using higher NaOH concentrations. In 1M NaOH solution, the WO_4^{2-} are eluted in the first desorption step, e. g. denoted as DES 1_1 in **Figure 6**, respectively. The results demonstrate that optimizing the NaOH concentration, the highest regeneration efficiency is enabled and in only 5min of reaction, therefore making the WO_4^{2-} recovery process possible.

Furthermore, it can be concluded that the initial NaOH concentration is playing an important role in the regeneration process, showing a maximum regeneration degree when the NaOH concentration is 1M. Further, 1M NaOH concentration was used to study the influence of salts addition in the regeneration solutions (**Figure 7**).

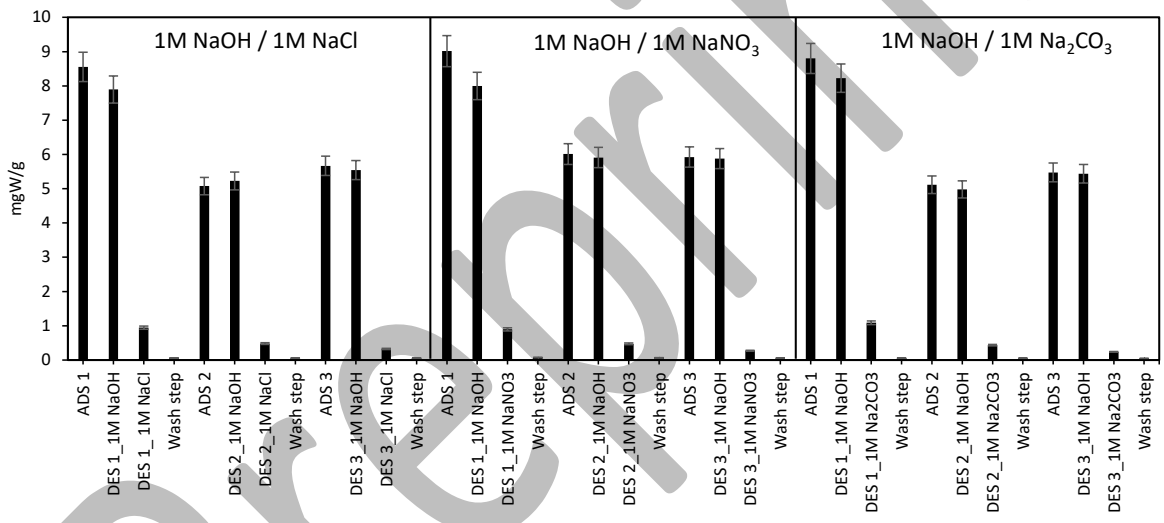

Figure 7. Desorption study in combination of 1M NaOH solution and different salts, where ADS stands for adsorption step (RT, S/L = 1g/L, contact time 120min and Ci of 100mgW/L) and DES stands for the desorption step (RT, S/L = 1g/L, contact time of 15min).

The results show that the presence of additional anions, such as Cl^-, NO_3^- or CO_3^{2-}, in the desorption solutions have an influence on the WO_4^{2-} elution but mainly in the first cycle, while the consecutives adsorption and desorption cycles are occurring with lower overall efficiency. In the first cycle approximately 9 – 10 mg W is adsorbed per g of LDH, from which ~85 % of W was eluted with 1M NaOH solution and the rest of ~15 % of W was eluted by the anionic exchange with Cl^-, NO_3^- or CO_3^{2-}, respectively. On the other hand, it is very important to mention that this positive effect of salts additions was observed only for the first cycle of

adsorption/desorption, and this is also why it was of great interest to study and optimize the regeneration process over multiple cycles. As the data included in **Figure 7** illustrates, the anions addition impacts the consecutive adsorption cycles, when the LDH capacity decreases from ~9 – 10 mg W/g LDH to only ~5 – 6 mg W/g of LDH, while the desorption degree remaining of its maximum efficiency with respect of WO_4^{2-} adsorbed per step.

3.4. Characterization of the solid phases after sorption – stability and mechanistic study

As described above, no specific difference was observed when using different salts during desorption trials, e.g. Cl^-, NO_3^- or CO_3^{2-}. Considering that the initial La-MgFe-LDH contains intercalated NO_3^-, the solids were recovered after the adsorption and desorption in NaOH and $NaNO_3$ solutions and characterized by means of XRD and IR measurements.

The desorption of any intercalated anion, and in the present case of WO_4^{2-}, from LDHs with high concentrations of NaOH and $NaNO_3$ can also cause structural changes to the LDHs. These structural changes are a consequence of the anionic exchange between the WO_4^{2-} anions with the HO^- and NO_3^- anions. This can be investigated by analyzing the shift of the (003) and (006) planes in XRD patterns, as well as the IR vibration bands corresponding to the different intercalated anions in the LDHs having multiple M – OH type of sites, due to the anionic exchange with different anionic sizes and hydration degrees.

The IR spectra and XRD patterns of La-MgFe-LDHs before and after WO_4^{2-} adsorption and desorption in NaOH or NaOH/$NaNO_3$ are shown in **Figure 8A** and **B,** respectively. In the IR spectra (**Figure 8A**) the main changes are occurring on the vibrations bands related with the M-OH bonds, namely in the regions above 3500cm^{-1} and below 800 cm^{-1} [49], while in the XRD patterns the main shifts are appearing in the basal planes (003) and (006) corresponding to the surface and interlayer changes, while no modification of the brucite-like layers can be observed [22].

The IR absorption band at 3648 cm^{-1} is attributed to the lattice vibration of M – OH in the LDHs layers (e.g. Mg – OH, Fe – OH and La – OH) [50]. It is important to note that this vibration band was present in the pristine La-MgFe-LDH (**Figure 8A, a**), while it was absent after WO_4^{2-} adsorption (**Figure 8A, b**) as well as after desorption in NaOH (**Figure 8A, c**), and further it only reappeared when a NaOH/$NaNO_3$ was used as a desorption solution (**Figure 8A, d).** This indicates that the WO_4^{2-} adsorption occurs on different sites with different strengths, e. g. interlayer anionic exchange of nitrates located at different M – OH groups.

These changes during the desorption study are indicating that the WO_4^{2-} anions are first released from the vicinity of Mg-OH sites ($WO_4^{2-} \Leftrightarrow NO_3^- \cdots HO - Mg$) while complete elution, mainly from the vicinity of the Fe-OH and La-OH groups is occurring in the presence of nitrate solutions ($WO_4^{2-} \Leftrightarrow NO_3^- \cdots HO - Fe$ or $WO_4^{2-} \Leftrightarrow NO_3^- \cdots HO - La$ (WO_4^{2-}). This later case is emphasized by the reappearance of the 3648 cm^{-1} adsorption band and the disappearance of the 665 cm^{-1} absorption band due to the nitrate exchange close to the Fe – OH and La – OH groups, respectively. This observation may be well correlated with previous reported literature studies, which indicate that below 1000 cm^{-1}, bands corresponding to the adsorbed tungstate species on LDHs are appearing, and thus their complete disappearance is an indication that the desorption is complete [25].

This observation was further confirmed by analyzing the IR spectra of the MgFe-LDH and La-MgFe-LDH in comparison with a MgAl-LDH synthesized under similar synthesis conditions (**Figure S4**). The absence of the absorption band at 3648 cm^{-1} in the MgAl-LDH correspondent and its presence in the MgFe-LDH sample clearly indicates that this is a characteristic of the Fe-LDHs, therefore referring to Fe – OH brucite-like groups in LDHs. Further, the 665 cm^{-1} absorption band may be assigned to the WO_4^{2-} absorbed on both Fe – OH and La – OH sites, as the combination of appearance of the 3648 cm^{-1} and concomitant disappearance of the 665 cm^{-1} occurs in the IR spectra after elution in first NaOH and followed by addition of $NaOH/NaNO_3$ solution, respectively.

Taking into account the capacity reduction after the first cycle, it can be concluded that the adsorption is occurring in proportion of ~85 % in the vicinity of Mg – OH sites, and ~15 % on the vicinity of the Fe – OH and La – OH sites, on the account of the anionic exchange. This approximation may be well correlated with the cationic ratio of M^{2+}/M^{3+} of 3/1 in the brucite like sheets. Further, the constant performances if the consecutive cycles might indicate that after the first desorption step, these ~15 % positions are rather very strongly exchanged and can't participate to the next adsorption and desorption steps, respectively, only a minor elution in the consecutive desorption steps may be observed.

The XRD patterns are also supporting the FT-IR conclusions, showing that especially the (006) plane shifts from 22° to 23° (2θ) after WO_4^{2-} adsorption and only returns on its original position after the nitrates are involved in the desorption process, indicating complete elution by anionic exchange of the WO_4^{2-} first with HO^- and secondly with NO_3^-.

These changes may be well correlated with the conclusions withdrawn from the desorption experiments when the desorption efficiency is decreasing after the first cycle, but further remains constant for the consecutive adsorption/desorption steps.

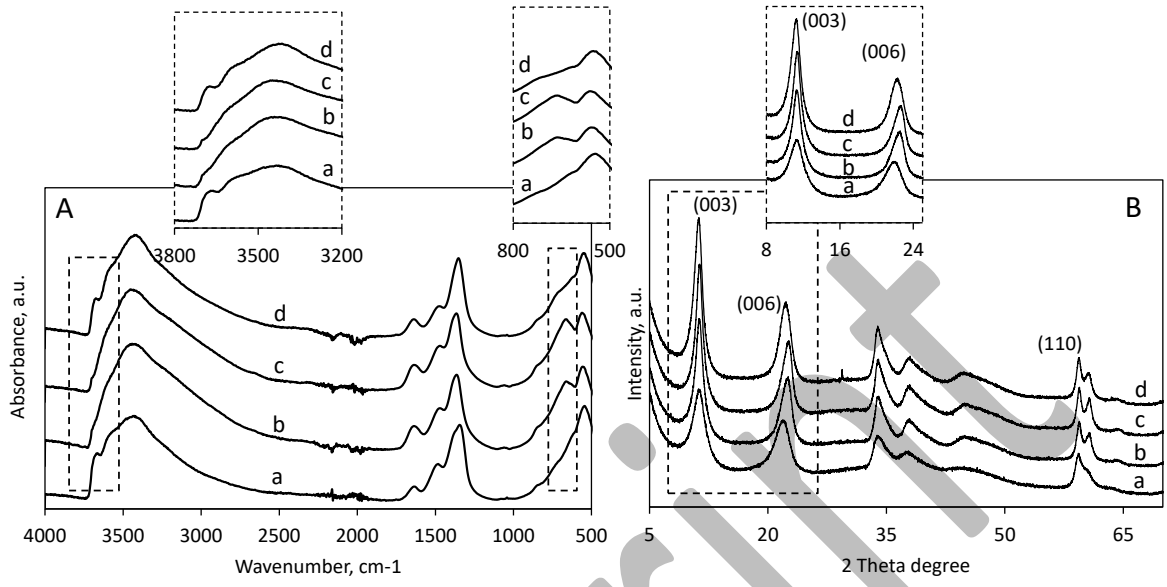

Figure 8. A: IR study and B: XRD study of (a) La-MgFe-LDH and (b) after WO_4^{2-} adsorption at pH 13 as well as after desorption in (c) 1M NaOH and (d) 1M $NaNO_3$, respectively. Insets: enlargements in the regions of interest as highlighted with dotted squares.

Furthermore, it should not be disregarded that these high alkaline NaOH solutions might also affect the crystallinity and structure integrity. It is well known that state-of-the art LDHs show stability issues when exposed to high pH media (pH ≥ 11) [38]. In the present study, the La-doping in the LDH structure assures the material stability as it was demonstrated using post characterization by XRD (**Figure 8B**) and its efficiency in the W adsorption/desorption process at such high pH values, namely pH 13 in the adsorption step and further pH 14 in the desorption step by using NaOH with concentrations ≥ 1. All these aspects related with material integrity due to high pH's can ultimately lead to a decrease in the overall performance of the LDH material, which in the present case was overcome by La-doping into the structure. This conclusion may be also well correlated with the results of stability tests included in **Figure S3**.

Overall, it may be concluded that the addition of salts in combination with NaOH is not necessary for the desorption of WO_4^{2-} anions from the LDHs.

NaOH solution with 1M concentration should be used for an efficient W desorption and a multicycle W recovery process is thus enabled. On the other hand, the second desorption cycle will start with a hydroxyl intercalated LDH, rather nitrate intercalated LDH, respectively. It can be concluded that, from the practical point of view, the addition of $NaNO_3$ solution is not necessary in combination with NaOH for the desorption of intercalated WO_4^{2-} anions from the La-MgFe-LDH during multicycle testing. NaOH alone can provide enough hydroxide ions to break the electrostatic interactions between the LDH layers and the anions, leading to their desorption.

4. Conclusions

In this study we focused on the synthesis of MgFe-LDH and its La-doped correspondent developed for the WO_4^{2-} recovery from highly alkaline solutions (pH ≥ 13). It is the first time that the development of an Fe-based LDH sorbent with an innovative structure by doping with La^{3+} cations within the brucite-type layers is reported. Such modifications assures the stability of the LDH at high alkaline media. Further, it improves the adsorption capacity in highly alkaline media as compared with a non-doped MgFe-LDH. The successful isomorphous substitution of La^{3+} into the brucite-like layers of the MgFe-LDH was demonstrated via X-ray diffractometry. The La^{3+} doped LDH shows increased unit cell parameters and improved its porosity characteristics, leading to unique anionic exchange properties and alkaline stability suitable for WO_4^{2-} recovery from alkaline solutions. The successful upscaling of the synthesis protocol to larger scale (20x) of the LDH with tailored structure doped with La^{3+} cations was demonstrated by X-ray diffraction and ICP analysis on the obtained powders, and this is for the first time demonstrated and reported up to our knowledge.

The WO_4^{2-} recovery was thoroughly investigated, with focus on parameters like LDH composition, adsorption capacity and kinetics. Further, the desorption step was optimized and multi-cycling tests in different desorption solutions combined with IR and XRD characterization of the La-MgFe-LDH solids in different steps of desorption, allowed us to elucidate the adsorption mechanism. The obtained results suggest that the as-developed La-MgFe-LDH show high potential to be applied in practice for WO_4^{2-} recovery from aqueous solutions, including highly alkaline solutions compatible with current hydrometallurgical processes.

CRediT authorship contribution statement

Seftel Elena M.: Writing – review & editing, Writing – original draft, Validation, Resources, Project administration, Methodology, Investigation, Funding acquisition, Formal analysis, Data curation, Conceptualization. **Spooren Jeroen**: Writing – review & editing, Methodology, Investigation, Conceptualization. **Kus Monika**: Formal analysis, Investigation, Validation. Cool Pegie: Conceptualization, Investigation, Methodology, Writing – review & editing**. Michielsen Bart:** Conceptualization, Funding acquisition, Investigation, Methodology, Resources, Writing – review & editing.

Declaration of Competing Interest

The authors declare the following financial interests/personal relationships which may be considered as potential competing interests: Elena M. Seftel, Jeroen Spooren, Bart Michielsen reports financial support was provided by EU Framework Programme for Research and Innovation Societal Challenges. Elena M. Seftel, Pegie Cool, Bart Michielsen have the patent METHOD FOR PRODUCING LANTHANIDEDOPED LAYERED DOUBLE HYDROXIDES issued to EP 3 502 058 A1.

Data availability

The authors are unable or have chosen not to specify which data has been used.

Acknowledgements

The authors acknowledge the TARANTULA project which received funding from the European Union's Horizon 2020 Research and Innovation program under Grant Agreement n°821159. This paper reflects only the author's views and neither Agency nor the Commission are responsible for any use that may be made of the information contained herein.

References

[1] D. Raabe, The Materials Science behind Sustainable Metals and Alloys, Chemical Reviews 123(5) (2023) 2436-2608.
[2] J. Bentley, S. Desai, B.P. Bastakoti, Porous Tungsten Oxide: Recent Advances in Design, Synthesis, and Applications, Chemistry 27(36) (2021) 9241-9252.
[3] E. Commission, Study on the Critical Raw Materials for the EU 2023, Final Report, Brussels, 2023, pp. 1 - 141.
[4] Y. Cao, Q. Guo, Z. Shu, C. Jiao, L. Luo, W. Guo, Q. Zhao, Z. Yin, Tungstate removal from aqueous solution by nanocrystalline iowaite: An iron-bearing layered double hydroxide, Environmental Pollution 247 (2019) 118-127.

[5] R.P.S. Gaur, Modern hydrometallurgical production methods for tungsten, JOM 58(9) (2006) 45-49.
[6] I.-H. Choi, G. Moon, J.-Y. Lee, R.K. Jyothi, Alkali fusion using sodium carbonate for extraction of vanadium and tungsten for the preparation of synthetic sodium titanate from spent SCR catalyst, Scientific Reports 9(1) (2019) 12316.
[7] J.F. Paulino, J.C. Afonso, J.L. Mantovano, C.A. Vianna, J.W. Silva Dias da Cunha, Recovery of tungsten by liquid–liquid extraction from a wolframite concentrate after fusion with sodium hydroxide, Hydrometallurgy 127-128 (2012) 121-124.
[8] D.S. Flett, Solvent extraction in hydrometallurgy: the role of organophosphorus extractants, Journal of Organometallic Chemistry 690(10) (2005) 2426-2438.
[9] X.-z. Zhu, G.-s. Huo, J. Ni, Q. Song, Removal of tungsten and vanadium from molybdate solutions using ion exchange resin, Transactions of Nonferrous Metals Society of China 27(12) (2017) 2727-2732.
[10] F. Di Natale, A. Lancia, Recovery of Tungstate from Aqueous Solutions by Ion Exchange, Industrial & Engineering Chemistry Research 46(21) (2007) 6777-6782.
[11] W.-C. Wu, T.-Y. Tsai, Y.-H. Shen, Tungsten Recovery from Spent SCR Catalyst Using Alkaline Leaching and Ion Exchange, Minerals 6(4) (2016) 107.
[12] H. Gecol, E. Ergican, P. Miakatsindila, Biosorbent for tungsten species removal from water: Effects of co-occurring inorganic species, Journal of Colloid and Interface Science 292(2) (2005) 344-353.
[13] I. Ihsanullah, M. Sajid, M. Kabeer, A.M. Shemsi, M.A. Atieh, First Investigations on the Removal of Tungsten Species from Water Using Multi-walled Carbon Nanotubes, Water, Air, & Soil Pollution 231(3) (2020) 119.
[14] T. Iwai, Y. Hashimoto, Adsorption of tungstate (WO4) on birnessite, ferrihydrite, gibbsite, goethite and montmorillonite as affected by pH and competitive phosphate (PO4) and molybdate (MoO4) oxyanions, Applied Clay Science 143 (2017) 372-377.
[15] Y. Cao, Q. Guo, W. Sun, G.A. Chelnokov, Efficient and Fast Removal of Aqueous Tungstate by an Iron-Based LDH Delaminated in L-Asparagine, International Journal of Environmental Research and Public Health 19(12) (2022) 7280.
[16] F. Ogata, Y. Iwata, N. Kawasaki, Properties of novel adsorbent produced by hydrothermal treatment of waste fly ash in alkaline solution and its capability for adsorption of tungsten from aqueous solution, Journal of Environmental Chemical Engineering 3(1) (2015) 333-338.
[17] F. Ogata, Y. Iwata, N. Kawasaki, Adsorption of Tungsten onto Zeolite Fly Ash Produced by Hydrothermally Treating Fly Ash in Alkaline Solution, Chemical and Pharmaceutical Bulletin 62(9) (2014) 892-897.
[18] F. Ogata, T. Nakamura, E. Ueta, E. Nagahashi, Y. Kobayashi, N. Kawasaki, Adsorption of tungsten ion with a novel Fe-Mg type hydrotalcite prepared at different Mg2+/Fe3+ ratios, Journal of Environmental Chemical Engineering 5(4) (2017) 3083-3090.
[19] L. Luo, Q. Guo, Y. Cao, Uptake of aqueous tungsten and molybdenum by a nitrate intercalated, pyroaurite-like anion exchangeable clay, Applied Clay Science 180 (2019) 105179.
[20] G. Lefèvre, J. Lion, A. Makolana, Extraction of tungsten as polyoxometalate anion using a layered double hydroxide: Selectivity and regeneration, Separation Science and Technology 54(4) (2019) 549-558.
[21] F. Cavani, F. Trifirò, A. Vaccari, Hydrotalcite-type anionic clays: Preparation, properties and applications, Catalysis Today 11(2) (1991) 173-301.
[22] E.M. Seftel, B. Michielsen, V. Meynen, S. Mullens, P. Cool, Insights into phosphate adsorption behavior on structurally modified ZnAl layered double hydroxides, Applied Clay Science 165 (2018) 234-246.
[23] E.M. Seftel, E. Popovici, M. Mertens, K.D. Witte, G.V. Tendeloo, P. Cool, E.F. Vansant, Zn–Al layered double hydroxides: Synthesis, characterization and photocatalytic application, Microporous and Mesoporous Materials 113(1–3) (2008) 296-304.

[24] K.A.C. Scott M. Auerbach, Prabir K. Dutta, Handbook of Layered Materials, Marcel Dekker, Inc., New York, 2004.
[25] A. Davantès, D. Costa, G. Lefèvre, Infrared Study of (Poly)tungstate Ions in Solution and Sorbed into Layered Double Hydroxides: Vibrational Calculations and In Situ Analysis, The Journal of Physical Chemistry C 119(22) (2015) 12356-12364.
[26] J. Olanrewaju, B.L. Newalkar, C. Mancino, S. Komarneni, Simplified synthesis of nitrate form of layered double hydroxide, Materials Letters 45(6) (2000) 307-310.
[27] S. Intasa-ard, M. Ogawa, Simple and cost-effective mass production of nitrate type MgAl layered double hydroxide: Titration from concentrated solution, Applied Clay Science 228 (2022) 106615.
[28] Elena M. Seftel, Bart Michielsen, Steven Mullens, Pegie Cool, Vera Meynen, METHOD FOR PRODUCING LANTHANIDE-DOPED LAYERED DOUBLE HYDROXIDES, Patent, EP 3 502 058 A1, 2017, pp. 1-26.
[29] M.I. Nave, K.G. Kornev, Complexity of Products of Tungsten Corrosion: Comparison of the 3D Pourbaix Diagrams with the Experimental Data, Metallurgical and Materials Transactions A 48(3) (2017) 1414-1424.
[30] G. Mishra, B. Dash, S. Pandey, Layered double hydroxides: A brief review from fundamentals to application as evolving biomaterials, Applied Clay Science 153 (2018) 172-186.
[31] R.W. Zhiping Zheng, RARE EARTH COORDINATION CHEMISTRY FUNDAMENTALS AND APPLICATIONS, John Wiley & Sons (Asia) Pte Ltd, Peking University, China, 2011.
[32] Y. Guo, Z. Zhu, Y. Qiu, J. Zhao, Adsorption of arsenate on Cu/Mg/Fe/La layered double hydroxide from aqueous solutions, Journal of Hazardous Materials 239-240 (2012) 279-288.
[33] E. Rodrigues, P. Pereira, T. Martins, F. Vargas, T. Scheller, J. Correa, J. Del Nero, S.G.C. Moreira, W. Ertel-Ingrisch, C.P. De Campos, A. Gigler, Novel rare earth (Ce and La) hydrotalcite like material: Synthesis and characterization, Materials Letters 78 (2012) 195-198.
[34] A. van Bommel, J.R. Dahn, Analysis of the Growth Mechanism of Coprecipitated Spherical and Dense Nickel, Manganese, and Cobalt-Containing Hydroxides in the Presence of Aqueous Ammonia, Chemistry of Materials 21(8) (2009) 1500-1503.
[35] J. Cho, LiNi0.74Co0.26-xMgxO2 Cathode Material for a Li-Ion Cell, Chemistry of Materials 12(10) (2000) 3089-3094.
[36] M.V. Bukhtiyarova, A review on effect of synthesis conditions on the formation of layered double hydroxides, Journal of Solid State Chemistry 269 (2019) 494-506.
[37] F. Rouquerol, J. Rouquerol, K. Sing, CHAPTER 6 - Assessment of Surface Area, Adsorption by Powders and Porous Solids, Academic Press, London, 1999, pp. 165-189.
[38] K.-H. Goh, T.-T. Lim, Z. Dong, Application of layered double hydroxides for removal of oxyanions: A review, Water Research 42(6–7) (2008) 1343-1368.
[39] J.W. Boclair, P.S. Braterman, Layered Double Hydroxide Stability. 1. Relative Stabilities of Layered Double Hydroxides and Their Simple Counterparts, Chemistry of Materials 11(2) (1999) 298-302.
[40] K.Y. Foo, B.H. Hameed, Insights into the modeling of adsorption isotherm systems, Chemical Engineering Journal 156(1) (2010) 2-10.
[41] I. Langmuir, THE ADSORPTION OF GASES ON PLANE SURFACES OF GLASS, MICA AND PLATINUM, Journal of the American Chemical Society 40(9) (1918) 1361-1403.
[42] W.J. Weber, Morris, J.C., Kinetics of adsorption carbon from solutions, Journal Sanitary Engineering Division Proceedings.American Society of Civil Engineers 89 (1963) 31-60.
[43] V. Fierro, V. Torné-Fernández, D. Montané, A. Celzard, Adsorption of phenol onto activated carbons having different textural and surface properties, Microporous and Mesoporous Materials 111(1–3) (2008) 276-284.
[44] S.S. S. Suresh, Green Chemical Engineering: An Introduction to Catalysis, Kinetics, and Chemical Processes, CRC Press2014.
[45] B.I. Olu-Owolabi, P.N. Diagboya, K.O. Adebowale, Evaluation of pyrene sorption–desorption on tropical soils, Journal of Environmental Management 137 (2014) 1-9.

[46] T.I. Atin Nuryadin, Ariyo Kanno, Koichi Yamamoto, Masahiko Sekine, Takaya Higuchi, Phosphate adsorption and desorption on two-stage synthesized amorphous-ZrO2/Mg–Fe layered double hydroxide composite, Materials Chemistry and Physics 266 (2021) 124559-124569.
[47] M.S. Asya Drenkova-Tuhtan, Karl Mandel, Carsten Meyer, Carsten Gellermann, Gerhard Sextl, Heidrun Steinmetz, Influence of cation building blocks of metal hydroxide precipitates ontheir adsorption and desorption capacity for phosphate inwastewater—A screening study, Colloids and Surfaces A: Physicochemical and Engineering Aspects 488 (2016) 145–153.
[48] Z.Z. Hong Jun, Lu Hongtao and Qiu Yanling, Effect of metal composition in lanthanum-doped ferric-based layered double hydroxides and their calcined products on adsorption of arsenate, RSC Advances 4 (2014) 5156-5164.
[49] E. M. Seftel, M. Mertens, P. Cool, E. F. Vansant, Infrared and Raman spectroscopic study of Sn-containing Zn/Al-layered double hydroxides, Journal of Optoelectronics and Advanced Materials 10(12) (2008) 3477-3481.
[50] Y. Song, Y. Tang, L. Fang, F. Wu, X. Zeng, J. Hu, S.F. Zhang, B. Jiang, H. Luo, Enhancement of corrosion resistance of AZ31 Mg alloys by one-step in situ synthesis of ZnAl-LDH films intercalated with organic anions (ASP, La), Journal of Magnesium and Alloys 9(2) (2021) 658-667.